STRUCTURAL DESIGN AND TESTING OF ACTIVE TWIST BLADES – A COMPARISON

J. Riemenschneider[1], S. Opitz[1], P. Wierach[1], H. Mercier des Rochettes[2], L. Buchaniek[2], D. Joly[2]

[1]German Aerospace Center (DLR), Lilienthalplatz 7, Braunschweig, Germany
[2]ONERA, 5, boulevard Painlevé, 59045 Lille, France

Abstract

Individual Blade Control (IBC) for helicopter main rotors promises to be a method to increase flight performance and to reduce vibration and noise. Several structural concepts for the implementation of such a secondary control have been presented in the past. Many of those include discrete mechanical components like hinges, levers or gears, which are subject to wear. In contrast to that, active twist blades use smart materials, which are directly embedded into the blade structure and – on top – do not show any discrete edges. Several different technologies have been proposed to twist rotor blades. Within the common DLR-ONERA partnership, a project called “Active Twist Blade” (ATB) was established in 2004, which investigated different concepts for active twist blades, using the BO105 blade with a cord length of 121 mm and a C-spar as reference.

The concept followed by DLR uses a technology consisting of skin integrated piezoelectric patches oriented at +/-45 deg in upper and lower skin, respectively. Specially shaped Macro Fiber Composite actuators (MFCs) generate a directed strain in the skin. This is a prerequisite for the shear torsion coupling, which causes the blade to twist. In addition to that the twist generation was enhanced by the use of non isotropy in the skin and a variation of the actuator orientation. Several different demonstrators have been designed and built, featuring different degrees of isotropy in the skin and different designs and angles of the actuator.

The concept followed by ONERA uses a twistable section closed by actuation (TWISCA), where the actuator is introducing warping into the section. This is done by cutting the section along the radius of the blade and bridging this gap with a shear actuator, which is causing the two sides of the slot to move parallel to one another. Different locations of the slot in the profile were proposed. At first a slotted trailing edge was investigated, where later developments move the slot into the spar region. Specially designed shear actuators – based on MFCs as well – were laid out to introduce the warping movement into the structure.

For both concepts several 1:2.5 Mach scaled demonstrator rotor blades were built which measure 2 m radius, each. Besides intensive lab tests for determining stiffness distribution and active twist for all blades a testing campaign in the DLRs whirl tower facility was carried out, which is especially equipped for testing rotor blades with active elements. The blades were tested in hover conditions, only. Blade tip twist was measured optically for all blades. The active twist angles for quasi static excitation exceeded the minimal demand of ±1.5 deg for all blades. On top of that the active twist under centrifugal loads and dynamic excitations was measured. The specific working capabilities of the designs were derived and compared, considering not only the twist at the blade tip, but also the torsional rigidity and the actuator volume. A first estimate for the power consumption of both active twist blades is made and issues like reliability and maintainability are discussed.

1. INTRODUCTION

Individual Blade Control (IBC) for helicopter main rotors promises to be a method to increase flight performance and to reduce vibration and noise. Several structural concepts for the implementation of such a secondary control have been presented in the past. Many of those include discrete mechanical components like hinges, levers or gears, which are subject to wear. In contrast to that, active twist blades use smart materials, which are directly embedded into the blade structure and – on top – do not show any discrete edges. Several different technologies have been proposed to twist rotor blades. Within the common DLR-ONERA partnership, a project called “Active Twist Blade” (ATB) was established in 2004, which investigated different concepts for active twist blades, using the BO105 blade with a cord length of 121 mm and a C-spar as reference.

2. STATE OF THE ART

The first active twist rotors using piezoceramic material incorporated in the aerodynamic relevant airfoil of the blade to change the twist were presented by Chen and Chopra from the University of Maryland. From 1993 to

1996 they built and hover tested a series of 1/8th Froude scaled model rotors. The rotor blade skins incorporated piezoceramic plates using the transversal piezoelectric d31-effect [1].

In 1995 a team joining researchers from Boeing, Penn State University and MIT started investigating in the field of active rotors. After proving the concept with a 1/16th Froude scale model rotor, they investigated the capability of active twist of two 1/6th Mach scale rotors (Active Material Rotor AMR). Since at this moment it was not sure whether the generation of structural twist or the twist generation via flaps is favorable, the first phase of this project included the design, manufacturing and testing of both design principles. At the beginning of the project the active twist concept was rated as the high risk approach whereas the flap design was considered to have low risk. This direct comparison by the same team of engineers developing both concepts side-by-side pointed out many advantages of the active twist concept. Actually the active twist concept turned out to be the low risk approach. Because of the encouraging results the active twist concept was applied to a modern planform and airfoil rotor blade. The active twist blades were actuated by interdigitated piezo fiber composites integrated in the spar of the rotor blade [2].
In 1999 a joint venture from NASA, Army and MIT built and tested an active twist rotor (ATR) with a structural design similar to the Boeing model rotor. This rotor was conceived for the testing in heavy gas medium, in the NASA Langley Transonic Dynamics Tunnel. This rotor is the only one which is wind tunnel tested under forward flight conditions. The twist is generated via Active Fiber Composite piezoelectric actuators embedded into the rotor blade spar [3-5].
In 2004 Boeing investigated the possibility of scaling the results of the Mach scaled rotor to a full scale rotor blade. The main focus of this investigation was laid on production and manufacturing approaches concerning the incorporation of the piezoelectric actuators and a robust and reliable wiring to provide the necessary power to the actuators. A 1.8m CH-47D blade section with 24 layers of active fiber composites embedded in the spar laminate was build and successfully tested. It was shown that a full scale active twist blade with a meaningful actuation capability and acceptable natural frequencies can be built within the weight limit of a passive blade [6].
Motivated by these promising results and the potential benefits DLR and ONERA established a common project called “Active Twist Blade” (ATB). The goal of this project is the design of twist blades that require as little energy as possible still showing good performance in twist. Whirl tower tests will not only show the quality of the blades under centrifugal loads, but also reveal possible problems in operation of the blades. The intention is to develop the necessary prerequisites for a successful wind tunnel campaign with an active twist model rotor.

3. DESIGNS FOR ACTIVE TWIST

Within the ONERA-DLR partnership, the “Active Twist Blade” (ATB) project was established in 2004 by a Joint Team. The investigations focused on two different concepts for active twist blades [7], using as reference the BO105 blade with NACA0012 airfoil. Final demonstrators for both concepts, presenting a chord of 121mm, were manufactured. The description of the concept as well as the design of the blades is presented in the following paragraphs.

3.1. DLR shear induced twist

The DLR concept is based on a principle of shear introduction - by means of piezoelectric actuators - into the blade skin, which causes the blade to twist. In general an introduction of strain in 45° direction causes a closed cell to twist. The main characteristics of the blades were taken from the well known BO 105 model rotor blade. The BO-105 blade features a C-Spar made of unidirectional glass fiber, a glass fiber skin and a foam core. The main difference between the original BO 105 model rotor and the blades developed and tested within ATB is that the original rotor is hingeless while the active twist blades are designed for a fully articulated rotor. This reduces the effort for the manufacturing of the blade and the rotor simulation on the one hand and allows proving the active twist principle on the other hand. The chord length of 121mm and the radius of 2m are in agreement with the original model rotor blade, whereas the profile was changed into a symmetrical NACA 0012, which does not really change the blade from a structural point of view. Also the blades are not pre-twisted.
The actuators that were used are Macro Fiber Composites (MFC), developed by NASA. Due to their particular electrode design these types of actuators have to be operated at relatively high voltages between -500 V and +1500 V to provide a sufficient electrical field.
The first demonstrator built at DLR (see Figure 1) is called AT1 and incorporated 2x11 standard MFC’s with 45° fiber direction. This results in an overall active area of approx. 1050cm². After the principle has been proven using the AT1 blade, several parameter studies for the optimisation of the skin lay-up were carried out [7]. The optimum found considers the twist deflection that can be achieved with respect to the torsional rigidity. The optimal configuration leads to a blade with an anisotropic skin. With regard to these findings the second model rotor blade (AT2) was built (see Figure 2). To provide a good coverage with active material and to realize the desired actuation direction of 40°, special shaped MFC actuators were designed for the AT2 blade. Two times six actuators were integrated into the rotor blade skins, resulting in a total active area of approx. 1600 cm².The actuator orientation was chosen to be +40°, whereas the skin was made of unidirectional glass fiber laminates with an orientation of -30° (inner skin). The area surrounding the actuators was provided with additional unidirectional glass fiber layers in a +40° direction (outer skin). The outer skin is used to carry the loads of the actuators and to

decrease the change in stiffness in the transition region between skin and actuators. The anisotropy of the skin allows the actuators to work in a relatively soft direction (approximately perpendicular to the fibers of the inner skin), whereas the complete blade still keeps its torsional stiffness by the shear stiffness perpendicular to the actuators.

The manufacturing process of the upper and lower blade skin started with the placement of the MFC actuators into the mould followed by the glass fiber prepreg. Accordingly the strain gauge instrumentation and the complete wiring were positioned onto the uncured prepreg. In the next step the lay-up was put in a vacuum bag and cured in an autoclave at a temperature of 120°C and a pressure of 6 bar. The spar and the foam core were machined to the desired shape using unidirectional glass fiber composite and foam blocks, respectively. Balancing weights made of tungsten rods were added into the nose of the spar using a cold setting epoxy. Finally the upper and lower skin, the spar and the foam core were bonded together with an adhesive film and cured at 120°C.

Figure 1: Actuator design of DLR blade AT1

Figure 2: Actuator design of DLR blade AT2

The Active Twist Blade was equipped with nine sets of strain gauges. Six sets were implemented for measurement of torsion (one for each actuator) and 3 for flapping. The locations of the strain gauges are shown in Figure 3. As described before the strain gauges and the necessary wiring were embedded into the blade skin during the manufacturing process. For each torsion measurement point, two strain gauges were arranged on opposite sides of the upper and lower blade shell in an angle of +/-45° degree to measure the torsional deformation of the blade. The individual strain gauges were wired to a full bridge to compensate for any bending deformation of the blade, so that only torsional deformations were measured. Since it is not possible to directly measure the twist angle with strain gauges, two additional acceleration sensors were mounted at the leading and trailing edge of the blade tip respectively. As backup and to check the results of the strain gauge and acceleration sensor measurements, a supplementary optical measurement system was installed. The system consists of two LED's attached at the leading- and trailing edge of the rotor blade tip and a stationary high speed camera system. By properly triggering the camera the twist movement of the blade can be visualized by the two light dots of the LED's. In comparison to a system that needs a powerful stroboscope light, capable of sufficiently illuminating the blade tip, this solution is much cheaper and also facilitates the analysis of the blade tip motion. Because the LED's appear as clearly distinguishable points, standard image processing tools can be used to automatically determine the twist angle.

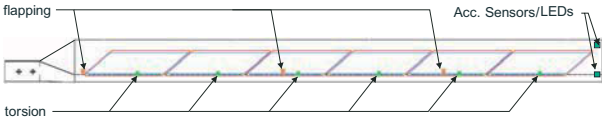

Figure 3: Sensor positions AT2

3.2. TWISCA

The name of the ONERA concept TWISCA stands for TWIstable Section Closed by Actuation. It is patented and based on the principle of an open blade section with a slot along the span direction, where the two edges of this slot are being connected by an actuation device. Actuating this device induces a relative translation movement in span wise direction of the upper and lower edges, resulting in warping of the structure, which leads to the twisting of the blade. In a first conceptual study the section was slotted at the trailing edge (see Figure 4). The shear actuator is attached to the lower and upper skin in the very end of the trailing edge (see Figure 5). As shown the forces resulting of the shear actuator are shifting the skins in span wise direction.

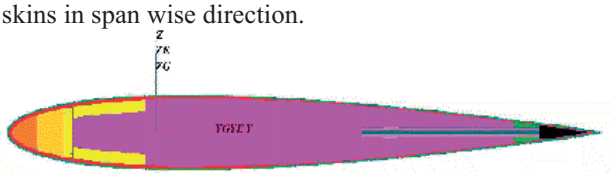

Figure 4: Section of 1st TWISCA design

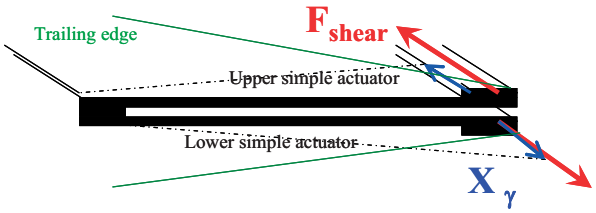

Figure 5: Design principle of TWISCA actuator

A demonstrator was designed and built, using this concept. The blade geometry consisted of an OA312 airfoil with a constant chord of 141.5mm and a span of 680mm at a rectangular plan form. The inner section consisted of a main spar that was made of partially unidirectional CFRP and, to adjust the cg and the neutral axis of the section at the quarter chord line, partially steel. In addition a tungsten balancing weight was added near the leading edge. This complex balancing concept was necessary because of the back position of actuation. This technology leads to a rather heavy structure which is not well suited for helicopter rotor blades, but the first objective was to check the feasibility of the concept.
The F.E. modelling of the blade structure was made with the assumption of the shear actuators being glued on both lower and upper side of trailing edge along a 570mm length.
In parallel, a technical investigation dealt with the study of the shear actuator to generate a push-pull movement inside the blade in the span direction. Different

"sandwich" combinations (ply numbers and orientations) of fabric and Macro Fiber Composite (MFC) purchased from Smart Material Corp. were tested in the lab. The actuator device choice was a good compromise between maximum shear strain and the minimization of longitudinal strain.

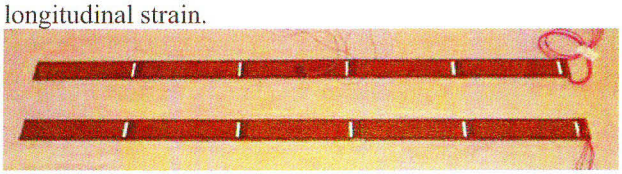

Figure 6: Two units of double shear actuator of pre-demonstrator

This choice led to a final design of the actuator, named "double actuator" (see Figure 6), adapted to the pre-demonstrator which consisted in the assembling of two simple shear actuators by gluing them together, this assembly being then connected to both trailing edge sides of the blade.

In the NASTRAN F.E. computations, the piezoelectric effect generated by the applied voltage on MFC's (-500/+1500V) is simulated by forces, the amplitudes of which were correlated with the shear deformation measured during preliminary lab tests performed on the chosen actuator in free conditions.

Eventually, the "double" actuator of the blade pre-demonstrator, made of 24 standard MFCs oriented at 45°, presenting an active surface of 571.2cm² of 570mm length, was manufactured and tested with a resulting shear deformation up to 1.07µm per applied volt.

The complete blade was tested in laboratory within a range of only –500/+1000V because of insulation issues. The experimental results (see Figure 7) confirmed F.E. simulation results about static twist performance at the tip of about ±0.68°/m (extrapolated to 2000Vpp) and allowed to validate the TWISCA concept applied to a real blade structure.

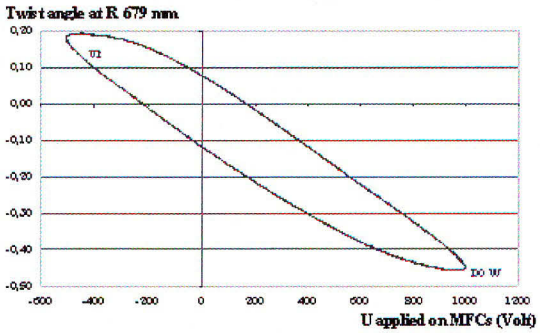

Figure 7: Quasi-static twist performance showing the hysteresis effect at R=679 mm

With the experience of this demonstrator, a second demonstrator was designed. Unlike the first one, the second one was supposed to have a cg at 25% chord, without adding too much extra balancing weight. This time the section is cut at the lower skin at 10% chord all throughout the blade length (see Figure 8). Again the previously described "double" actuators (see Figure 6) were used. Two units, 750 mm each have been implemented. Due to the risk of sparks in the actuator the driving voltage was reduced to -500V to +1000V.

The calculated mechanical blade characteristics are very close to those of the BO 105 model rotor blade (for more details see [8]).

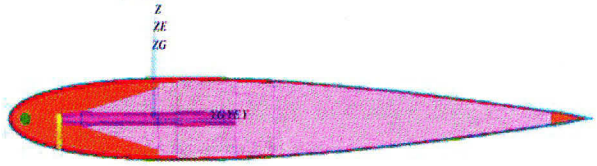

Figure 8: Section of 2nd TWISCA design

The final demonstrator was at first tested in the lab to assess its mechanical behavior without centrifugal or aerodynamic loads. The torsional stiffness GJ was examined by application of a torsional moment M_T and measurement of the resulting angel θ in a distance l of the clamp.

$$GJ = \frac{M_T * l}{\theta}$$

It turned out, that the torsional stiffness was over 30 % below the design stiffness – as well as the torsional frequency. More detailed investigations of the blades dynamics can be found in [8]. This very same demonstrator was also tested in the DLR whirl tower facility, to evaluate the twist performance under centrifugal loads.

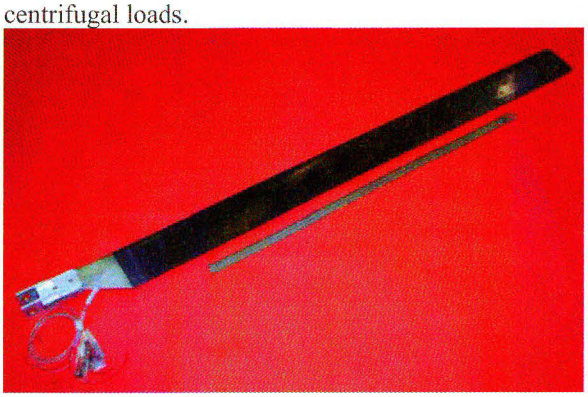

Figure 9: Final TWISCA demonstrator

4. TESTING OF DEMONSTRATORS

Both blades have been tested in the DLR whirl tower facility, which allows centrifugal tests of rotor blades up to R=2m without cyclic pitch.

4.1. Test setup

The objective of the test was the demonstration of the performance of the actuation systems and the structural concepts under centrifugal loads by showing that the expected twist deformation can be achieved at the nominal rotation speed and different actuation frequencies. For this purpose a test rig was installed at the DLR rotor tower in Braunschweig (see Figure 10)[9]. The test rig is driven by a 47kW DC motor. A balancing weight is mounted on the opposite side to trim the blade. To reduce the mechanical complexity the pitch links have been removed and the pitch angle has been fixed. The

blade is mounted articulated in flap and lead lag. Data transfer is realized by 24 slip rings and an additional telemetry system with 12 channels for strain gauge measurements (full bridge or half bridge) and 4 ICP channels for acceleration sensors. Four special designed high voltage slip rings transfer the required electrical power to the actuators in the blade. Depending on the excitation frequency the actuators were driven with up to three power amplifiers with a peak to peak voltage of 2000V and a maximum current of 400mA.
In order to analyze the blade tip twist, a high speed camera was installed, which takes pictures of the LEDs, which are attached at the blade tip. The optical analysis of these pictures allows an online measurement of the twist angle at the azimuth of the camera location.

4.2. Blade testing

During the testing campaigns several properties of the blades were investigated. On one hand the eigenfrequencies of the blades under centrifugal loads were investigated. For this purpose a voltage sweep was applied to the actuators to excite the blade. Since this was done at different rotor speeds, a fan plot could be derived. Additionally the influence of the centrifugal forces to the quasi static active tip twist was checked.
On the other hand for nominal rotor speed the twist amplitude at different higher harmonic excitations was investigated.

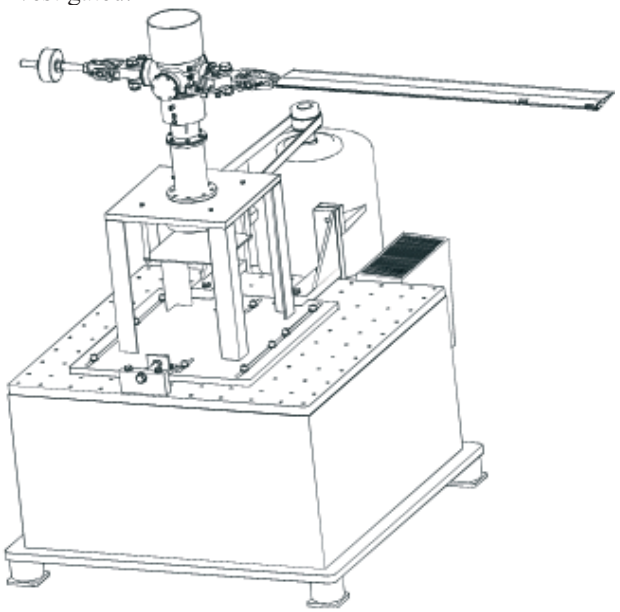

Figure 10: Centrifugal test rig

4.3. Testing of TWISCA

The demonstrator (Figure 9), instrumented with flap and torsion strain gauge bridges (three stations), was tested during a first campaign under centrifugal forces on the DLR test rig (Figure 16) up to 960rpm without any breakdown.

Figure 11: TWISCA demonstrator in DLR whirl tower

However, an increasing noise appeared in the sensors output signals, which was not observed in the lab tests before. This was most likely an EMC problem - generated by the actuator current, due to a bad ground connection between the blade structure made of carbon fiber and the whole electrical test rig equipment. Despite the difficulties to analyse the test data, the static twist could be considered similar to that without any load.
In a second campaign the demonstrator was equipped with additional 9 flap-torsion hybrid bridges (half flap and half torsion) for SPA measurement (Strain Pattern Analysis [10]) of the blade deformation and with two LEDs located at the blade tip. The strain gauges as well as the wires were glued to the outside of the skin. The wires were located as much as possible at the trailing edge. Also two LEDs were glued to the blade tip. Resulting tip twist angles can be found in Figure 12. Unfortunately, there was an electrical failure in one of the actuators after the measurements at 750rpm, which finished the experiments early. Right now there is no technique to repair the built in actuators.

4.4. Testing of DLR blades

The individual wiring of each actuator segment of the AT2 allows the actuation of individual blade regions [9]. It could be shown, that depending on the excited frequency it might be beneficial not to excite all actuators at the same phase, but rather to switch some of them off [11]. In order to compare the results between the DLR and ONERA active twist blade the results of quasi static excitation can be used. Switching off some of the actuators is not beneficial for quasi static excitation. For this reason all actuators are operated. As sensing units the LED measurements have been used only.
Even though the maximum operation voltage of the actuators was reduced from 1500V to 1300V, there were some electrical failures in the actuators during the testing of the DLR-blades as well. But there is one main difference to the ONERA blade and to all former active twist blades incorporating piezoceramic fiber actuators, the actuators are integrated in the rotor blade skin and they are easily accessible. Hence in case of a burn out failure the actuator can be repaired without a big delay in the testing or even worse a loss of the whole actuator. The repair procedure is very easy and fast. At first the failure is milled out until there are no residua of carbon from the

electric arc of the failure. To ensure the insulation the hole is filled with an epoxy resin. Since the burn outs are usually very small only a narrow stripe of the actuator becomes inactive. For this reason there is only a very small decrease in twist authority even in case of a failure. After some small failures the blade achieved a stable state and the whole test campaign could be made almost without interruption.

5. COMPARISON

5.1. Comparison of test results

There are many ways how the twist capability of active rotor blades can be compared. One of them is just the active twist at different excitation frequencies. Since the scale of the investigated blades is equal, it is an easy approach to just measure the tip twist angle at different excitation frequencies (see Figure 12). Since the nominal rotor speed of the two blades is slightly different, the exact frequencies for the higher harmonics do not really match for the two blades.

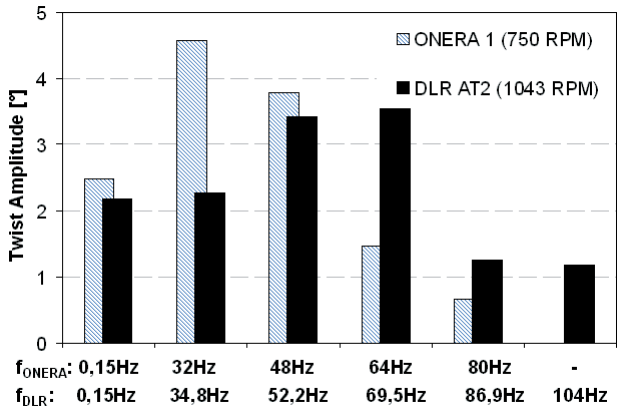

Figure 12: Tip twist angles of DLR and ONERA blade

It can be seen, that the ONERA blade shows a slightly higher twist amplitude and also a much earlier decrease of the amplitude, which is caused by the first torsional eigenfrequency. Whereas the DLR blade shows its eigenfrequency around 4/rev, the TWISCA blade is around 2/rev. The reason for this deviation is the difference in stiffness and mass distribution of the two blades. The TWISCA blade seems to be little heavier and not quite as stiff, as the baseline BO105 blade [8]. Further comparisons of active rotor blades need some more considerations [12].

The comparison of active twist rotor blades is nontrivial. Even though the blades have similar scale, there are huge differences in actuator design and implementation. Also, it is not reasonable to compare the twist angles without regarding the torsional stiffness of the blade or the twist frequency. When the twist frequency approaches the eigenfrequency of torsion the twist amplitude is only depending on the damping of the system. This means almost any amplitude can be reached. Since the natural frequencies of the different blades are varying, the only reliable actuation frequency is located in the range of quasi static excitation. Nevertheless it is possible to compare the different blades if the right performance values are calculated. The procedure for the calculation of a representative performance value is described in [12] and needs only four characteristic blade values:

1. quasi static active tip twist angle, Φ_{model} [rad]
2. length of active region, L_{model} [m]
3. torsional stiffness of the model blade, GI_{model} [Nm²]
4. volume of active piezoceramic material, V_{model} [m³]

When model blades are downscaled from full scale using the dimensionless scaling factor S the following typical scaling laws can be applied:

- $\Phi_{full} = \Phi_{model}$
- $L_{full} = S \cdot L_{model}$
- $GI_{full} = S^4 \cdot GI_{model}$
- $V_{full} = S^3 \cdot V_{model}$

Since it is important to evaluate the twist angle under consideration of the torsional stiffness, the generated active twist moments are a good indicator of the blades twist capabilities. The moments of model scale and full scale blades can be calculated as follows:

$$M_{model} = \frac{GI_{model}}{L_{model}} \cdot \Phi_{model}$$

$$M_{full} = \frac{GI_{full}}{L_{full}} \cdot \Phi_{full} = \frac{S^4 \cdot GI_{model}}{S \cdot L_{model}} \cdot \Phi_{model}$$

$$M_{full} = S^3 \cdot M_{model}$$

Thus it appears that comparison of the moments would have a cubic dependence from the scaling factor and is therefore not suited. The working capabilities of model and full scale blade differ by the same factor and can be calculated as follows:

$$W_{model} = \frac{1}{2} \cdot M_{model} \cdot \Phi_{model}$$

$$W_{full} = \frac{1}{2} \cdot M_{full} \cdot \Phi_{full} = \frac{1}{2} \cdot S^3 \cdot M_{model} \cdot \Phi_{model}$$

$$W_{full} = S^3 \cdot W_{model}$$

As it is easy to understand that the twist capability will rise when more active material is used a representative performance value can be found by calculating the working capability referred to the volume of active material used in the rotor blade. The result is a kind of specific working capability, w [J/m³].

$$w_{model} = \frac{W_{model}}{V_{model}}$$

$$w_{full} = \frac{W_{full}}{V_{full}} = \frac{S^3 \cdot W_{model}}{S^3 \cdot V_{model}} = w_{model}$$

When using the scaling laws mentioned above, the specific working capability is a measure of the performance of the blades completely independent from the scale of the model blade used for the experimental investigation. Table 1 shows the characteristic values needed to calculate the specific working capabilities of the active twist blades described earlier.

	AT1	AT2	TWISCA
GI_{model}	156 Nm²	194 Nm²	110 Nm²
Φ_{model}	3,48°	3,94°	4,6°
V_{model}	21,6cm³	32,2cm³	31,4cm³
L_{model}	1.755m	1.755m	1.755m

Table 1: Characteristic values of active twist blades

According to these considerations the active twist blades were compared by means of the specific working capability (see Figure 13). It can be shown, that the specific work capabilities of all three blades are in the same order of magnitude. The shear induction into the skin seems to be a little more effective, especially the use of unidirectional fibers, which reduces the stiffness in the direction of the actuators slightly, shows a great performance. Regarding the TWISCA concept, the difference in the stiffness of skin (carbon fiber in contrast to the DLR blades made of glass fibers) and actuator material could have caused some of the slightly reduced working capabilities.

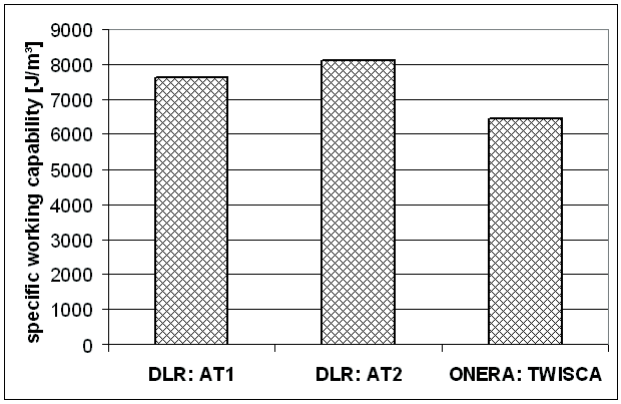

Figure 13: Specific working capability of DLR and ONERA blades

5.2. Comparison of estimated power consumption

Since the goal of the ATB project is to develop an active twist rotor which consumes as little power as possible a method to make a realistic estimate of the power consumption has to be developed. Before starting the estimation it has to be kept in mind that there are some minor differences in the nominal speed of the two blades. As the ONERA blade is spinning approx. 8% slower than the AT2 the power values are generally a little bit smaller since the power is proportional to the frequency for capacitive loads. Further on the testing of the ONERA blade was performed at 750rpm while the AT2 was tested at 1043rpm but this should be of minor importance and is just mentioned for the reason of completeness. The power consumed by an active twist rotor blade is depending on the desired tip twist angle, the twist frequency and the dynamic characteristics of the blade (see Figure 12). To predict the power needed to drive an active twist rotor in a realistic manner it is sensible to assume a certain control law for the twist motion of the blade tip. This control law is the outcome of a rotor simulation and can be adapted to minimize noise or vibration in different flight conditions. For the evaluation of the electrical power needed to operate the active twist blades the optimized control laws for minimum vibration at different flight speeds provided by AgustaWestland within the European project Friendcopter were used. The control laws were developed for the Friendcopter model rotor blade and hence not accounting for the maximum achievable twists of the AT2 or the TWISCA blade. The control law is composed by sine functions of different frequency, amplitude and phase. The frequency is always a multiple of the rotational frequency of the rotor (2/rev – 5/rev). Since the excitation frequencies used to generate these tip twists were already used to determine the tip twist in the whirl tower test, the gain of the transfer function converting voltage to tip twist can be used to predict the voltage signal needed to generate the desired tip twist. This can be only done under the condition of a linear system. Due to the fact that the optical measurement was not synchronized to the measurement of the actuator voltage at the time of the measurement campaign, it was only possible to determine the gain of the transfer function from voltage to tip twist. Later on an enhancement of the measurement system allowed measuring the phase shift between the signals too. For the following calculations the phase shift is assumed to be zero which has only minor influence on the determination of the control law for the actuator voltage.

The second simplification is that the voltage amplitude which is theoretically needed to achieve the tip twist described by the control law at a certain frequency is not limited for this simple comparison. This corresponds to the fact that the maximum achievable tip twist was not considered within the determination of the control laws. Consequently the actuator voltage can exceed the upper and lower limit of the operating limits of the actuators. Nevertheless the calculated power values can be used for a qualitative comparison of the blades. Using the characteristics measured in the whirl tower and the control laws for different flight speeds describing the tip twist motion, the actuator voltage for the ONERA blade and the AT2 can be calculated. Figure 14 shows the actuator voltage needed to achieve the tip twist to minimize the vibration at a forward speed of 40kts.

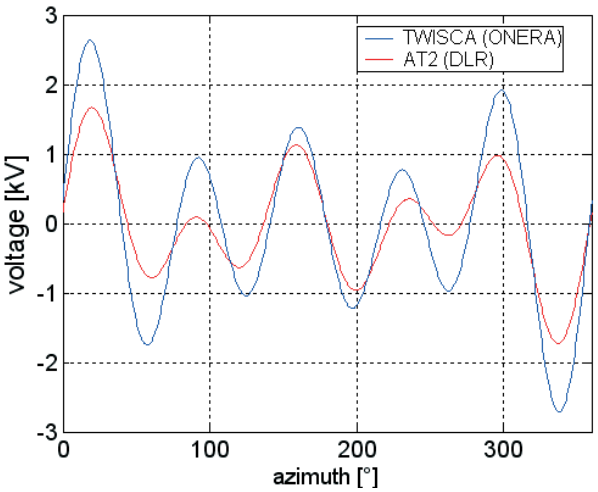

Figure 14: Voltage law to minimize vibration at 40kts forward speed

Due to the higher frequency contents of the control law and the smaller tip twists of the ONERA blade at those frequencies the voltage to drive the ONERA blade is higher than for the AT2. Especially at high frequencies this is disadvantageous since the power is proportional to the squared voltage and the frequency for capacitive loads like MFCs. As the piezoceramic actuators of the active twist blade have mainly capacitive behavior it is important to note that a certain amount of electric energy is stored in the actuators. This energy is not necessarily lost. Hence it has to be distinguished between effective power, reactive power and apparent power. The apparent power has to be considered when the amplifiers are chosen. The effective power is the minimum power that is needed to operate the blade. The reactive power is the power which results from the energy stored in the actuators and can be partially recovered using smart amplifiers.

In the first step of the estimation of the power consumption the control law for the actuator voltages was calculated using the control law for the tip twist and the amplitude responses of the experimentally derived transfer functions that relate tip twist and voltage.

The second step is the characterization of the electrical behavior of the blades. Since both voltage and current were recorded during the experiment the impedance respectively the admittance of the system can be determined for the excitation frequencies of interest. Knowing the admittance of the system the current response to the voltage excitation can be calculated easily. Once again a linear system is assumed. Knowing the voltage and the current signal, the complex power can be calculated for each of the signals frequency contents. Afterwards the effective and the apparent power at different frequencies can be summed up to predict the power of the complete signal. Please note that all presented power values are not including the losses in the generator and the amplifiers. The effective power to drive the active twist blades can be seen in Figure 15.

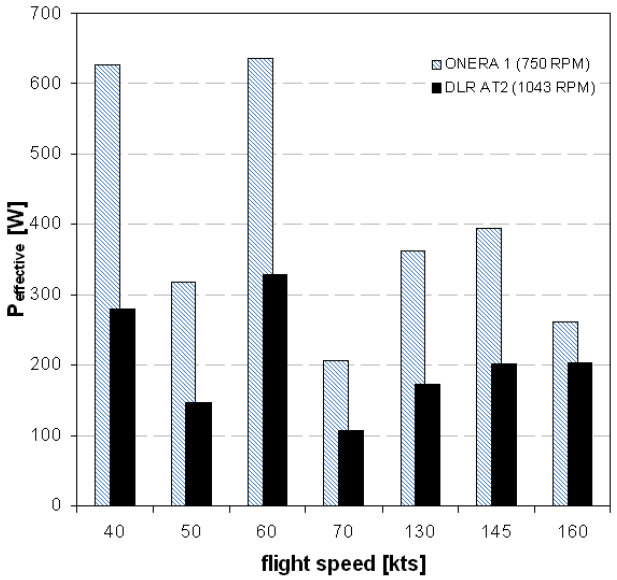

Figure 15: Effective power for vibration reduction at different flight speeds

The next step would be to estimate the power needed to drive a 4 bladed full scale active twist rotor. For this estimation some scaling laws have to be used. To achieve the same tip twist angle in full scale, it is necessary to scale up area and thickness of the actuators. Hence the amount of active material is scaled up with the scaling factor to the power of three (S^3). Since the power needed is proportional to the volume of active material it would also be scaled with S^3 but since the model rotors are Mach scaled (same Mach number at the blade tip) the rotational frequency of the full scale rotor equals the rotational frequency of the model scale rotor divided by the scaling factor. As the power is proportional to the frequency it can be stated that the power has to be scaled with S^2. This value has to be multiplied with the number of blades. Figure 16 shows the estimated effective power of a 4 bladed full scale rotor.

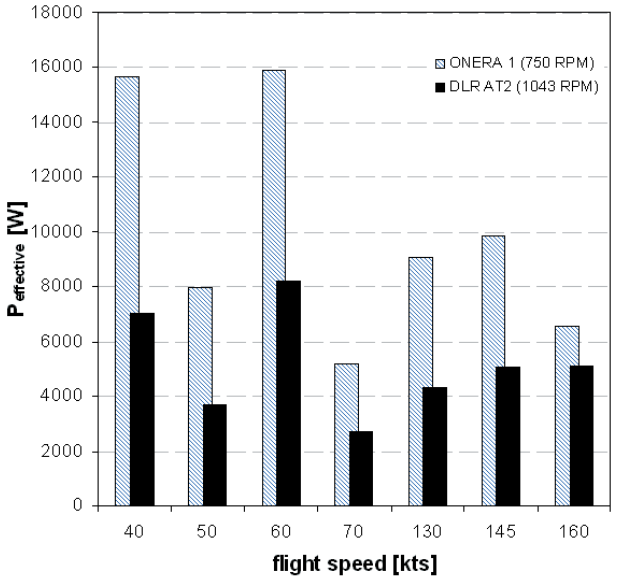

Figure 16: Estimated power to minimize vibration for a full scale 4 bladed active twist rotor

The estimated power values show the impact of the rotor blade dynamics. Even though the TWISCA blade had slightly better performance up to 3/rev the power to drive the blade in a minimum vibration mode is much higher than the power needed for the AT2 blade. This is due to the high frequent contents of the minimum vibration control law. This first comparison using the minimum vibration control law can only give a first hint on how to design an efficient active twist rotor blade. When other control laws as for example a minimum noise control law, are used the higher tip twist in the low frequency range can be advantageous.

6. PLANNED ACTIVITIES

Both concepts are currently developed further with the goal of a wind tunnel experiment within the next 3 years.

7. CONCLUSION

Two totally different concepts for the generation of active twist have been developed into model scale demonstrators. One is using shear introduction into the blade skin, the other one uses a cut section, which is filled by actuation. Both concepts have proven to work even under centrifugal loads. Within this work the specific working capability of the demonstrators has been calculated and shown, that those measures were rather close for both concepts. It seems that the shear introduction shows somewhat better results, since the stiffness correlation between actuator and passive structure match better.
Further on the power consumption was estimated for both blades. The slightly higher twist authority of the DLR blade at frequencies above 3/rev reduces the power consumption significantly when the control law has no restrictions on the amplitude for those frequencies.
The experimental investigations have also shown some difficulties that will be coming up in operation such as failure safety. Even though there are strong activities towards the development of better (in terms of electrical shortages) actuators, there has to be a repair concept for any active twist blade that will be operated with a real helicopter.

8. ACKNOWLEDGMENTES

The authors from DLR would like to thank the EU for partial funding of this work in the framework of the FRIENCOPTER project.
The authors from ONERA would like to thank the French Civil Aviation Authorities and DGA for their support to blade model structure design.

Bibliography

[1] I. Chopra, "*Status of Application of Smart Structures Technology to Rotorcraft Systems*," *Journal of the American Helicopter Society*, vol. 45, no. 4, pp. 228-252, 2000.

[2] R. Derham, D. B. Weems, M. B. Mathew, and R. C. Bussom, "The design evolution of an active materials rotor," American Helicopter Society, 2001.

[3] S. Shin, C. E. S. Cesnik, and R. Hall, "*Closed-Loop Control Test of the NASA/ARMY/MIT Active Twist Rotor for Vibration Reduction*," Phoenix, Arizona, USA: 2003.

[4] M. L. Wilbur, W. T. Yeager, W. K. Wilkie, C. E. S. Cesnik, and S. Shin, "Hover Testing of the NASA/ARMY/MIT Active Twist Rotor Prototype blade," American Helicopter Society, 2000.

[5] M. L. Wilbur, P. H. Mirick, W. T. Yeager, C. L. Langston, C. E. S. Cesnik, and S. Shin, "Vibratory Loads Reduction Testing of the NASA/ARMY/MIT Active Twist Rotor," Washington, DC: American Helicopter Society, 2001.

[6] D. B. Weems, D. M. Anderson, M. B. Mathew, and R. C. Bussom, "*A Large-Scale Active-Twist Rotor*," Baltimore, MD, USA: 2004.

[7] J. Riemenschneider, S. Keye, P. Wierach, and H. Mercier des Rochettes, "Overview of the Common DLR/ONERA Project 'Active Twist Blade'," Marseille: 30th European Rotorcraft Forum, 2004.

[8] H. Mercier des Rochettes, B. Junker, L. Buchaniek, and P. Leconte, "A New Concept of Active Twist Blade applied to Main Rotor of Helicopter," Evora, Portugal: 2009.

[9] P. Wierach, J. Riemenschneider, S. Opitz, and F. Hoffmann, "Experimental Investigation of an Active Twist Model Rotor Blade under Centrifugal Loads," Kazan, Russia: 2007.

[10] N. Tourjansky and E. Széchényi, "The measurements of blade deflections a new implementation of the strain pattern analysis," Avignon: 13th ERF, 1992.

[11] F. Hoffmann, S. Opitz, and J. Riemenschneider, "Validation of Active Twist Modeling Based on Whirl Tower Tests," Grapevine, Texas, USA: American Helicopter Society International, 2009.

[12] H.P.Monner, S.Opitz, J.Riemenschneider, and P.Wierach, "Evolution of Active Twist Rotor Designs at DLR," Schaumburg, USA: 2008.